Molecular Orbital Imaging of the Acetone S_2 Excited State Using Time-Resolved (*e*, 2*e*) Electron Momentum Spectroscopy

Masakazu Yamazaki,[1] Keiya Oishi,[1] Hiroyuki Nakazawa,[1] Chaoyuan Zhu,[2] and Masahiko Takahashi[1,*]

[1]*Institute of Multidisciplinary Research for Advanced Materials, Tohoku University, Sendai 980-8577, Japan*
[2]*Department of Applied Chemistry, Institute of Molecular Science, National Chiao-Tung University, Hsinchu 30050, Taiwan*
(Received 3 December 2014; published 13 March 2015)

We report a time-resolved (*e*, 2*e*) experiment on the deuterated acetone molecule in the S_2 Rydberg state with a lifetime of 13.5 ps. The acetone S_2 state was prepared by a 195 nm pump laser and probed with electron momentum spectroscopy using a 1.2 keV incident electron beam of 1 ps temporal width. In spite of the low data statistics as well as of the limited time resolution (± 35 ps) due to velocity mismatch, the experimental results clearly demonstrate that electron momentum spectroscopy measurements of short-lived transient species are feasible, opening the door to time-resolved orbital imaging in momentum space.

When a molecule in the ground state absorbs a photon of light of the appropriate wavelength, the molecule is raised to an electronically excited state. Such molecular excited states are usually short lived, as they may subsequently undergo, within a short period of time, unimolecular deactivation reactions involving isomerization, dissociation, radiative, nonradiative, and energy-transfer processes. Furthermore, since the energies of the electronic excitation are on the order of chemical bond energies, molecules in excited states are more reactive than those in their ground state. Indeed a lot and variety of chemical reactions in which molecular excited states participate can be found in literature [1]. For these reasons, the study of excited-state molecular structures and dynamics is a topic of growing interest owing to the fundamental importance as well as potential application in many areas [2].

With the above mentioned background, there have been a number of proposals and even some excellent experiments that have sought to investigate the nature of molecular excited states. For instance, time-resolved x-ray absorption spectroscopy, exploiting short laser and x-ray pulses in a pump-probe scheme, has evolved to an established technique to achieve electronic structure information about excited states of molecules [3]. As well, the time-resolved electron/x-ray diffraction technique has made it possible to visualize the geometrical structures of transient species [4–6]. Nevertheless, there still remains the challenge that is to experimentally look at molecular orbitals in excited states. It is their spatial distributions that largely determine various physical and chemical properties of the excited molecules such as bonding, reactivity, and molecular recognition [7].

The use of an advanced form of electron momentum spectroscopy (EMS) is a potentially possible way to realize such orbital imaging of excited molecules. EMS is an experimental technique that has been developed, over the last four decades, as a powerful means to measure momentum density distributions of each electron bound in matter or to look at spatial distributions of electron orbitals in momentum space [8–10]. In spite of its potential, however, application of EMS has been limited to studies on stable targets in their ground state, except the early pioneering experiment of Zheng *et al.* [11] on excited sodium atoms prepared by using a continuous-wave ring dye laser. This is partly due to the difficulty of performing EMS experiments that require the coincident detection of the two outgoing electrons produced by high-energy electron-impact ionization at large momentum transfer, where the (*e*, 2*e*) reactions generally have quite small cross sections compared with those at small momentum transfers. Furthermore, use of an ultrashort-pulsed incident electron beam, which is the primary requirement of conducting EMS experiments for short-lived transient species, imposes an additional difficulty; if the intensity of the ultrashort-pulsed incident electron beam is increased, space charge effects may disturb the measurements by significantly broadening not only the temporal width but also the energy spread of the electron packet [12]. Under these circumstances, we have very recently developed a time-resolved EMS (TR-EMS) apparatus [13] based on the latest technological achievement in the instrumental sensitivity for traditional EMS [14].

In this Letter we report the first application of TR-EMS to an excited molecule. Here, the deuterated acetone (acetone-*d*6) molecule, $(CD_3)_2CO$, in its second excited singlet S_2 (*n*, 3*s*) Rydberg state with a lifetime of 13.5 ps [15] has been chosen as the target. Although the statistics of the data are unsatisfactory, the measured (*e*, 2*e*) binding energy spectra and spherically averaged electron-momentum-density distribution are consistent with the expected nature of the acetone-*d*6 S_2 state. The present work can thus be recognized as having demonstrated the feasibility of EMS measurements of short-lived molecular excited states.

The experiment on the acetone-*d*6 S_2 state was carried out using the TR-EMS apparatus. Since details of the

apparatus are described elsewhere [13], only a brief account of it is given here. Figure 1 shows a schematic representation of the experimental setup. The 800 nm output of a 5-kHz femtosecond laser (<120 fs, 0.8 mJ) was split into a pump path and an electron-generation path. 90% of the output was used to yield with an optical parametric amplifier the pump laser pulse (195 nm, ∼120 fs, 0.8 μJ), which was subsequently used to excite acetone-$d6$ molecules in a target gas beam to the S_2 state after the 5-kHz repetition rate being halved by an optical chopper. On the other hand, 10% of the 800 nm output was frequency tripled by a third harmonic generator and it was directed toward a back-illuminated photocathode, after being attenuated as required (267 nm, <10 μJ), in order to produce electron pulses via the photoelectric effect. The photocathode was made of a silver film of 40 nm thickness, which was negatively biased to accelerate the electron pulses up to 1.2 keV. The resulting ultrashort pulsed electron beam (1.2 keV, ∼1 ps, ∼50 pA) was then used to induce EMS events. The delay time t_{delay} between the arrival of the pump laser pulse and the probe electron pulse was controlled with a computer-driven translation stage. The EMS events were recorded by an EMS spectrometer for which an exceptionally large spherical analyzer (mean radius of 220 mm) was employed.

For the EMS measurements, the symmetric noncoplanar geometry was employed (Fig. 1), in which two outgoing electrons having equal energies and making equal scattering angles ($\theta_1 = \theta_2 = 45°$) with respect to the incident electron beam axis were detected in coincidence.
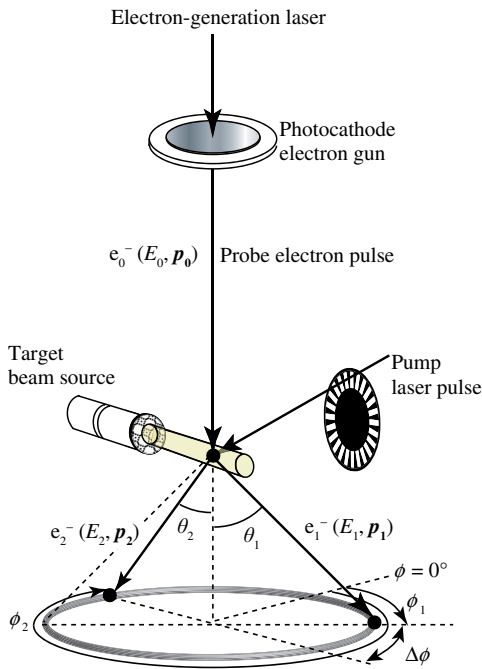

FIG. 1 (color online). A schematic representation of the experimental setup for time-resolved symmetric-noncoplanar $(e, 2e)$ experiments.

The binding energy (E_{bind}) and momentum (p) of the target electron, before ionization, can be determined through the following energy and momentum conservation laws [8–10]:

$$E_{\text{bind}} = E_0 - E_1 - E_2, \quad (1)$$

$$\boldsymbol{p} = \boldsymbol{p}_1 + \boldsymbol{p}_2 - \boldsymbol{p}_0. \quad (2)$$

Here E_j's and $\boldsymbol{p}_j$'s ($j = 0, 1, 2$) are kinetic energies and momenta of the incident, inelastically scattered, and ejected electrons, respectively. In this kinematic scheme, the magnitude of the target electron momentum p is given by

$$p = \sqrt{(p_0 - \sqrt{2}p_1)^2 + [\sqrt{2}p_1 \sin(\Delta\phi/2)]^2}, \quad (3)$$

with $\Delta\phi$ being the out-of-plane azimuthal angle difference between the two outgoing electrons detected.

The TR-EMS measurements for the acetone-$d6$ S_2 state were carried out at delay times t_{delay} of 0 and 100 ps, while accumulating data at ambient sample gas pressure of 1.3×10^{-4} Pa for 18 days and 31 days runtime, respectively. Here, in order to have a workable signal count rate, diameters of the target gas beam, the pump laser, and the probe electron beam were all set to be about 2 mm. However, the use of such large diameter beams brought about at the same time lowering of the energy, momentum, and time resolution and they were 5 eV FWHM, 0.4 a.u. at $\Delta\phi = 0°$, and ± 35 ps, respectively. Note that the time resolution is almost entirely dominated by the group velocity mismatch between the pump laser and the probe electron beam [16]. Note also that since the 5-kHz repetition rate was halved only for the pump laser, the TR-EMS apparatus concurrently produced two kinds of EMS data sets. One is data that were measured with the pump laser (laser-on). The other is reference data that were measured without the pump laser (laser-off) and hence they are equivalent to traditional EMS data for the ground state molecule.

Figure 2 shows the laser-on and laser-off binding energy spectra thus obtained at $t_{\text{delay}} = 0$ ps, which were constructed by plotting the number of true coincidence events summed up over the entire covered $\Delta\phi$-angle range as a function of the binding energy (E_{bind}). Also included in the figure is an associated theoretical spectrum for the acetone-$d6$ ground state, which was created in the following manner: The most widely used scattering model for EMS is the plane-wave impulse approximation with the weak-coupling approximation [8–10] that describes EMS cross sections as

$$\frac{d^3\sigma_{\text{PWIA}}}{dE_1 d\Omega_1 d\Omega_2} \propto S_\alpha \frac{1}{4\pi} \int d\Omega |\psi_\alpha(\boldsymbol{p})|^2. \quad (4)$$
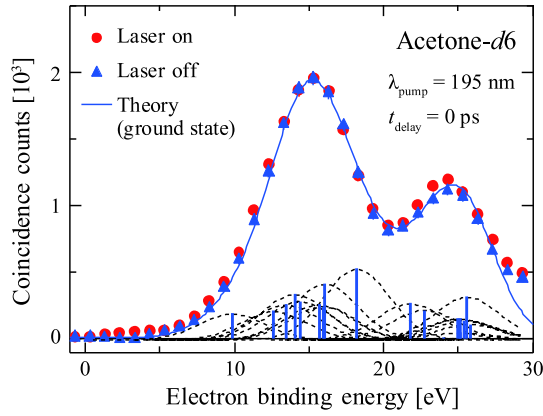
FIG. 2 (color online). Experimental laser-on and laser-off EMS binding energy spectra of the acetone-$d6$ molecule obtained at a delay time t_{delay} of 0 ps. The broken and solid lines represent associated theoretical calculations for the laser-off spectrum. See text for details.

Here, $\psi_\alpha(\boldsymbol{p})$ is the momentum-space representation of the quasiparticle or Dyson orbital. S_α is a quantity called pole strength. $(1/4\pi)\int d\Omega$ is the spherical averaging due to random orientation of gaseous targets. In the present calculations, the Dyson orbitals for each ionization transition were approximated by Kohn-Sham orbitals [17] generated with the density functional theory. Their binding energies and pole strength values were taken from the theoretical study of Zheng et al. for the acetone ground state [18], except that the former values for the inner-valence ionizations were employed by being lowered by 1–2 eV so as to reproduce the laser-off spectrum while keeping the main-satellite energy separation of the poles unchanged. The associated theoretical spectrum was then obtained by assuming each ionization transition had a Gaussian profile with a width of the instrumental energy resolution (5 eV FWHM) and by summing up their contributions.

It can be seen from Fig. 2 that although the poor instrumental energy resolution does not allow the spectral peaks to be identified clearly, the laser-off spectrum is on the whole well reproduced by the associated theoretical spectrum over the entire binding energy range covered. It can also be seen from the figure that the laser-on spectrum shows small but noticeable differences from the laser-off spectrum. Since both the spectra were measured concurrently by accumulation of data for 18 days runtime, it is possible to hardly attribute the origin of the observed differences to drifts in the electron beam current and/or fluctuations in the target gas density. It is shown below in terms of both the binding energy spectrum and the spherically averaged electron-momentum-density distribution that the observed differences are because of the effect of the 195 nm pump laser employed, that is, contributions of EMS events from the acetone-$d6$ S_2 state.

Figure 3(a) shows a TR-EMS binding energy spectrum of the acetone-$d6$ S_2 state, measured at $t_{delay} = 0$ ps. This
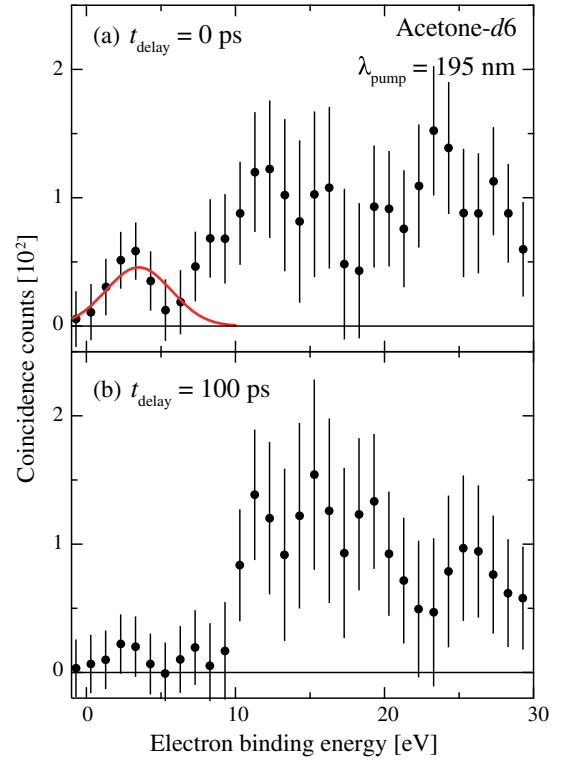

FIG. 3 (color online). Experimental time-resolved EMS binding energy spectra of the acetone-$d6$ S_2 state obtained at delay times t_{delay} of (a) 0 ps and (b) 100 ps. The solid line represents a band due to ionization from the outermost $3s$ Rydberg orbital.

spectrum was generated by subtracting the laser-off spectrum with a weight factor of 0.95 from the laser-on spectrum in Fig. 2, in order to remove contributions from the S_0 ground state. The difference of the weight factor from unity (0.05) represents the possibility of the acetone-$d6$ S_2 state existing in the molecular ensemble. The weight factor of 0.95 was chosen so as to be the maximum value under constraint that any data point in the resulting TR-EMS spectrum should not exhibit an intensity less than zero, though the weight factor value is a bit smaller than our estimate based on the absolute photoabsorption cross section of the acetone molecule [19] and the pump laser power used. Note, however, that the argument made below is not affected by the choice of the weight factor value.

It is evident from Fig. 3(a) that a band appears at around $E_{bind} = 3.5$ eV. It should be noted that the value of 3.5 eV is much smaller than the lowest ionization potential (9.8 eV) of the ground-state acetone molecule [18] and hence this band cannot appear in the laser-off spectrum. Furthermore, by keeping in mind that the photon energy of the employed 195 nm pump laser is 6.36 eV, the band at around 3.5 eV is undoubtedly assigned, from consideration of energy conservation, to ionization from the outermost $3s$ Rydberg orbital of the acetone-$d6$ S_2 excited state. In addition, the 3.5 eV band disappears when the delay time

t_{delay} is changed from 0 ps to 100 ps, as can be seen from Fig. 3(b) where a TR-EMS binding energy spectrum at $t_{delay} = 100$ ps, generated in the same way with the same weight factor value of 0.95, is shown. This is indeed in accordance with the fact that the acetone-$d6$ S_2 state has a lifetime of 13.5 ps and it undergoes the three-body ultrafast dissociation process to eventually produce 2CD$_3$ and CO [15], indicating that the $t_{delay} = 100$ ps spectrum is largely governed by the reaction products. These observations confirm us in unwavering confidence that a successful EMS measurement of a molecular excited state has been achieved.

Further evidence for the successful measurement is given by examining angular correlation between the two outgoing electrons detected. Figure 4 shows spherically averaged electron-momentum-density distribution for the 3s Rydberg orbital, which was constructed by plotting the number of true coincidence events that formed the 3.5 eV band as a function of the electron momentum. Also included in the figure are associated theoretical distributions calculated in two different ways. One (DFT_3s Ryd.) is the distribution generated by using an empty Kohn-Sham orbital of the acetone-$d6$ S_0 state and the other (CASSCF_3s Ryd.) is that generated by using a 3s orbital of the S_2 state optimized with the complete-active-space self-consistent-field method [20]. In addition, a theoretical distribution for the outermost bound orbital of the S_0 state (DFT_S_0 HOMO) is included as a reference to highlight the behavior of the 3s Rydberg orbital. All three theoretical distributions are height-normalized to the experimental maximum intensity at $p = 0.05$ a.u.,

although the first two are almost indistinguishable from each other.

It can be seen from Fig. 4 that although the statistics of the data leave much to be desired, the experimental result exhibits a maximum at the momentum origin and its intensity drops off rapidly with the increase in the electron momentum. This behavior can be understood by considering in momentum space the nature of the 3s Rydberg orbital. Since the angular part of a wave function is invariant under the Dirac-Fourier transform, a certain molecular orbital in position space has similar shape in momentum space. On the other hand, the radial part of a wave function is largely affected by the Dirac-Fourier transformation; high density at large r leads to high density at small p and vice versa. Thus the diffuse 3s Rydberg orbital possesses the sharply peaked momentum distribution. The two associated theoretical calculations support this observation.

In summary, the present work reported the TR-EMS experiment on the acetone-$d6$ S_2 state with the lifetime of 13.5 ps. The experimental binding energy spectra and spherically averaged electron-momentum-density distribution have represented the first time that EMS measurements of molecular excited states are feasible, opening the door to time-resolved orbital imaging of various short-lived transient species in momentum space. However, there is ample room for improvements, mainly in data statistics and energy and time resolution. Generally speaking, the signal intensity of TR-EMS is proportional to the product of the number of the molecular ensemble N_{mol} and the intensity of the pump laser I_{pump}. In the present TR-EMS apparatus, a continuous target gas beam is used and N_{mol} is limited by the size and capacity of the employed vacuum pumps. This strongly suggests that provided a commercially available pulse nozzle with an opening time of 7 μs and the 5 kHz repetition rate is employed, N_{mol} is expected to be increased by a factor of 28.6 or more [21]. Similarly, I_{pump} can also be increased, for instance by more than 10 by use of a latest version of current commercially available laser systems. The energy and time resolution of TR-EMS could also be improved by reducing the incident electron beam current and by making the size of the interaction region smaller along the incident electron propagation direction, respectively, thereby in a trade-off relationship with the signal intensity. In addition, the disadvantage and advantage of TR-EMS compared with other, potentially possible time-resolved orbital imaging techniques may also have to be noted. For example, the tomographic imaging technique with laser-induced tunnel ionization and high-harmonic generation has demonstrated its excellent ability to observe spatial distributions of molecular orbitals in the three-dimensional form and in position space [22,23]. As compared with an advanced form of this technique, TR-EMS must be inferior in data statistics and time resolution. However, TR-EMS has advantages in its ability to conduct measurements, based on the well-established EMS collision
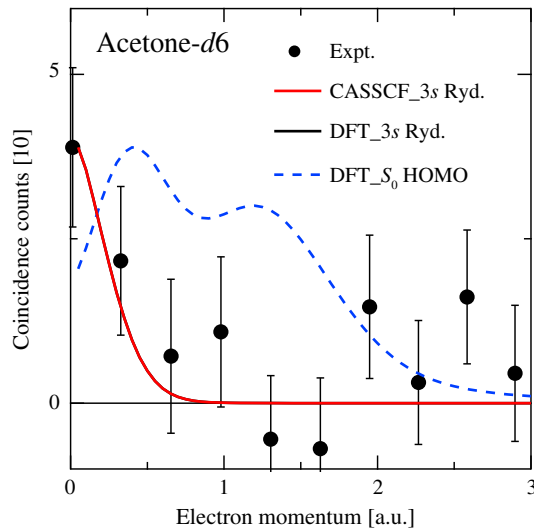

FIG. 4 (color online). Comparison of spherically averaged electron-momentum-density distributions between experiment and theory for the 3s Rydberg orbital of the acetone-$d6$ S_2 state. A theoretical distribution for the outermost orbital of the acetone-$d6$ S_0 state is also shown by the broken curve as a reference to highlight the behavior of the 3s Rydberg orbital.

physics with a long history, in a laser-field-free condition with rigorous orbital selection using the energy conservation law for not only one or a few outermost orbitals but also all other, more tightly bound orbitals. With these further technical developments and the methodological advantages, we expect TR-EMS would exploit a new area for studies of ultrafast molecular dynamics as well as the nature of molecular excited states.

[*] masahiko@tagen.tohoku.ac.jp

[1] N. J. Turro, *Modern Molecular Photochemistry* (University Science Books, Sausalito, USA, 1991).

[2] *Applied Photochemistry*, edited by R. C. Evans, P. Douglas, and H. D. Burrows (Springer, New York, 2013).

[3] L. X. Chen, Annu. Rev. Phys. Chem. **56**, 221 (2005).

[4] A. H. Zewail, Annu. Rev. Phys. Chem. **57**, 65 (2006).

[5] R. J. D. Miller, R. Ernstorfer, M. Harb, M. Gao, C. T. Hebeisen, H. Jean-Ruel, C. Lu, G. Moriena, and G. Sciaini, Acta Crystallogr. Sect. A **66**, 137 (2010).

[6] J. Kim, K. H. Kim, J. H. Lee, and H. Ihee, Acta Crystallogr. Sect. A **66**, 270 (2010).

[7] K. Fukui, Science **218**, 747 (1982).

[8] E. Weigold and I. E. McCarthy, *Electron Momentum Spectroscopy* (Kluwer Academic/Plenum, New York, 1999), and references therein.

[9] M. A. Coplan, J. H. Moore, and J. P. Doering, Rev. Mod. Phys. **66**, 985 (1994).

[10] M. Takahashi, Bull. Chem. Soc. Jpn. **82**, 751 (2009).

[11] Y. Zheng, I. E. McCarthy, E. Weigold, and D. Zhang, Phys. Rev. Lett. **64**, 1358 (1990).

[12] B. J. Siwick, J. R. Dwyer, R. E. Jordan, and R. J. D. Miller, J. Appl. Phys. **92**, 1643 (2002).

[13] M. Yamazaki, Y. Kasai, K. Oishi, H. Nakazawa, and M. Takahashi, Rev. Sci. Instrum. **84**, 063105 (2013).

[14] M. Yamazaki, H. Satoh, M. Ueda, D. B. Jones, Y. Asano, N. Watanabe, A. Czasch, O. Jagutzki, and M. Takahashi, Meas. Sci. Technol. **22**, 075602 (2011).

[15] J. C. Owrutsky and A. P. Baronavski, J. Chem. Phys. **110**, 11206 (1999).

[16] J. C. Williamson and A. H. Zewail, Chem. Phys. Lett. **209**, 10 (1993).

[17] P. Duffy, D. P. Chong, M. E. Casida, and D. R. Salahub, Phys. Rev. A **50**, 4707 (1994).

[18] Y. Zheng, J. J. Neville, C. E. Brion, Y. Wang, and E. R. Davidson, Chem. Phys. **188**, 109 (1994).

[19] P. J. Singh, A. Shastri, B. N. R. Sekhar, R. D'Souza, and B. N. Jagatap, J. Quant. Spectrosc. Radiat. Transfer **114**, 20 (2013).

[20] B. O. Roos, in *Advances in Chemical Physics; Ab Initio Methods in Quantum Chemistry–II*, edited by K. P. Lawley (John Wiley & Sons Ltd., Chichester, England, 1987).

[21] M. Yamazaki, Y. Kasai, K. Oishi, H. Nakazawa, and M. Takahashi, J. Phys. Conf. Ser. **488**, 012056 (2014).

[22] J. Itatani, J. Levesque, D. Zeidler, H. Niikura, H. Pépin, J. C. Kieffer, P. B. Corkum, and D. M. Villeneuve, Nature (London) **432**, 867 (2004).

[23] C. Vozzi, M. Negro, F. Calegari, G. Sansone, M. Nisoli, S. De Silvestri, and S. Stagira, Nat. Phys. **7**, 822 (2011).